Test and Simulation of Basalt Fiber Steel Tubes Concrete

Zhishuo Yang[1, 2]

[1]*College of Civil Engineering and Architecture, Central South University, Changsha 410081, Hunan, China*
[2] *College of Civil Engineering, Putian University, Putian 351100, Fujian, China*

Yezhi Zhang

College of Civil Engineering and Architecture, Central South University, Changsha 410081, Hunan, China

Abstract
This paper present test and numerical model for short steel tube columns filled with ultra high strength concrete and basalt fiber reinforced concrete under axial load. The study aimed to explore the effect of basalt fiber on the behavior of concrete-filled steel tube (CFST) columns with ultra high strength concrete. Three specimens were tested with basalt fiber volume percentages of 2kg/m^3, thicknesses of steel tube of 4mm and concrete strengths 0f over 100 MPa. At the same time, three dimensional nonlinear FE analysis of axial compression, was conducted using the finite element program ABAQUS/Standard solver. The results indicate that the presence of basalt fiber has obvious effect on the ultimate load of CFST columns. And the numerical results were validated through comparison with experimental data in terms of axial loading.
Key words: BASALT FIBER, SUPER HIGH STRENGTH CONCRETE, STEEL TUBES, BEHAVIOR AND NUMERICAL SIMULATION

1. Introduction

Concrete-filled steel tubular columns (CFST) are gaining increasing usage in modern construction practice, offering increased load carrying capacity, but without occupying greater floor area. The origin of concrete-filled tubular columns can be traced back to 1879 when they were first used for the piers in the Severn railway bridge in the UK. Further investigations, most notably in Russia, Western Europe, North America and Japan, took place during the 1960s, but construction difficulties, particularly associated with concrete pouring, resulted in limited uptake, and usage was largely architecturally driven. However, developments in pumping techniques and high strength concrete in the 1980s heralded a rapid increase in the use of CFST columns in high-rise buildings, longspan bridges and heavy industrial buildings. A review of developments in the use of concrete filled tubes in construction has been carried out by Shanmugan and Lakshmi [1,13].

Basalt fibers are produced from basalt rocks, which are melted at 1400 C. Basalt fibers are environmentally safe, non-toxic, and possess high stability and insulating characteristics [14-15]. Basalt Fiber has been recently introduced as an alternative to Steel fiber for concrete structures. Unlike Carbon Fiber Reinforced Polymer (CFRP) and Glass Fiber Reinforced

Polymer (GFRP) materials, basalt fibers have not been widely used. Chopped basalt fibers have been also introduced as an additive to concrete mixes to produce fiber reinforced concrete (FRC).[16-17] No one is study of the basalt fibers on the short steel tube columns filled with high strength concrete.

The research presented in this paper comprises two main studies. The first, we conducted experimental tests to investigate the reinforcing effect of basalt fibers on the short steel tube columns filled with high strength concrete. A finite element model was developed through the ABAQUS/standard solver to predict the axial compressive resilience of the ultra-high strength concrete-filled steel tubular columns secondly.

2. Experimental program

2.1. Material properties

Cement. The cement used in this paper was type II ordinaryPortland cement (grade 42.5) purchased from Fujian wangnianqing Cement Company. The chemical compositions and physical properties of cement used are given in Table 1.

Supplementary cementing materials. The silica fume, a by-product of silicon metal in a powder form, was used in the production of SHSCUS, the properties of which is shown in Tables 1.

Fly ash .Class A fly ash, a by-product of thermal power stations, was used in these experiments, and the chemical property of fly ash was shown in Tables 1.

Figure 1. Basalt fiber

Fiber. Basalt fiber used mainly in concrete and mortar was used in these experiments. As the Figure.1 shows

Superplasticizer. The polycarboxylic-acid type superplasticizer (TW-PS) (abbreviated to SP)was used in these tests.

Aggregate. Locally available crushed stone with a nominal maximum size of 15 mm was used as coarse aggregate, and river sand of Qingkou was used as fine aggregate.

Table 1. Properties of material

Component	Cement(%)	Silica fume(%)	Fly ash(%)
SiO2		93.47	
SO3	≤3.5		1
MgO	≤5	0.47	
Fe2O3		0.24	
CaO		0.30	0.6
K2O		0.48	
Na2O		0.23	
Al2O3		0.30	
CI+	≤0.06		
Loss on ignition	≤5	3.47	3
Water		0.68	0.56

The measured unconfined compressive cube strengths for concrete grades see table 2, respectively. Table 3 shows the measured dimensions and material properties of the circular hollow sections. In order to study the convenient, the B specimen loaded will be modeled in this paper.

Table 2. Mix of extra-high strength concrete mixed with stone-chip

Mix								
Cement	Silica fume	Fly ash	sand	Crushed stone	Superplasticizer	Water-binder ratio	basalt fiber	f_{cu}
Kg	Kg	Kg	Kg	Kg	Kg	%	Kg	MP_a
380	65	200	610	1150	8	0.21	2	100

Where, f_{cu} = compressive strength(Standard test block:150*150*150)

Table 3. Parameters of specimens

Specimen number	$D\times t$	D/t	L	L/D	f_y
	mm		mm		MP_a
B	120.0×4.0	30	740	3.3	235

Where, D= outer diameter of steel tube, t = thickness of the steel pipe, L= length of steel tube, f_y =yield strength of steel tube.

2.2. Specimen preparation

A stiffened end cap of 10 mm was attached at the base of each steel tube. The concrete was filled without any vibrations, and then the specimens were left to cure in the laboratory for about 28 days. Prior to testing, the top surface of concrete core was roughened with a wire brush and a thin layer of high strength cement was poured on the roughened surface. This procedure was adopted to minimize the effect of concrete shrinkage so that the steel tube and the concrete core can be loaded simultaneously during testing.

Figure 2. Test set up

2.3. Test set-up and instrumentation

To understand the basis of the numerical modeling method and assess the accuracy of the numerical simulations, it is necessary to provide a description of the physical tests and the main experimental observations. All tests were performed in a YAW-800 column testing machine at College of Civil Engineering of Putian University. For each test specimens, axial load, axial displacement from the test machine comes with software to automatically capture. Axial lateral strain through DH3818 static strain gauge automates data acquisition and storage by a computer and the data acquisition frequency is 3 times per second. The test set-up is shown in Figure.1. While minute eccentricities might occur, every effort has been made to reduce the effect of the eccentric loading to ensure that the columns were concentrically and uniformly loaded.

The tests were conducted using a universal testing machine with a capacity of 8000 kN. The test arrangement is shown in Figure.2. The load was applied in an increment of 50 kN before peak load. Each load interval was maintained for 2–3 min. The load was slowly applied near and after the peak load to investigate the post-peak behavior of the specimens. Two linear variable differential transducers (LVDTs) were located vertically to measure the axial shortening of the specimens. Eight strain gauges were placed at the

mid-height of the steel tube to measure the vertical deformation and perimeter expansion at four symmetric locations.

3. Test results and discussions

3.1. Failure modes and test observations

After the external Basalt tube is removed, an obvious shear plane in concrete is found to exist among the bulges, as shown in Figure.3. The formation of the major diagonal crack contributes to axial load drop. The force transfer through shear-friction on the cracked surfaces is the main mechanism for plain concrete of maintaining the resistance to the applied axial load. Those columns, especially with high strength concrete, experienced a sudden loss of axial load.

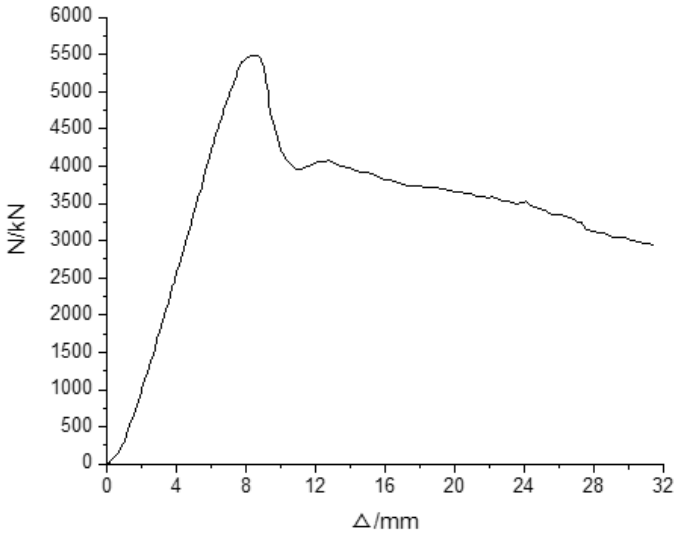

Figure 3 Axial load (N) versus end shortening (Δ).

Figure 4 Failure modes of specimens

3.2. Ultimate load

The maximum load during loading is defined as the ultimate load. The ultimate loads of the specimens are shown in Figure. 4. The effects of the concrete strength and the thickness of steel tube on the ultimate load of the basalt fiber reinforced concrete-filled steel tub specimens are as expected: adding Basalt fibers into concrete had slight effect on the ultimate load of the CFST specimens.

4. Finite element (FE) model

The FE model developed through the ABAQUS/Standard solver will be used to simulate the concrete-filled circular steel stub columns under axial compression.

Figure.3 shows a typical FE model in which three-dimensional 8-node solid elements (C3D8) were adopted for both the elliptical steel hollow section and the confined concrete core. Considering the effects of other factors on the predicted structural behavior in numerical models, such as the stub column dimensions, appropriate mesh size would be 5–10 mm for the steel hollow section and 10–20 mm for the concrete, i.e. the concrete element size is about twice the element size of the steel hollow section.

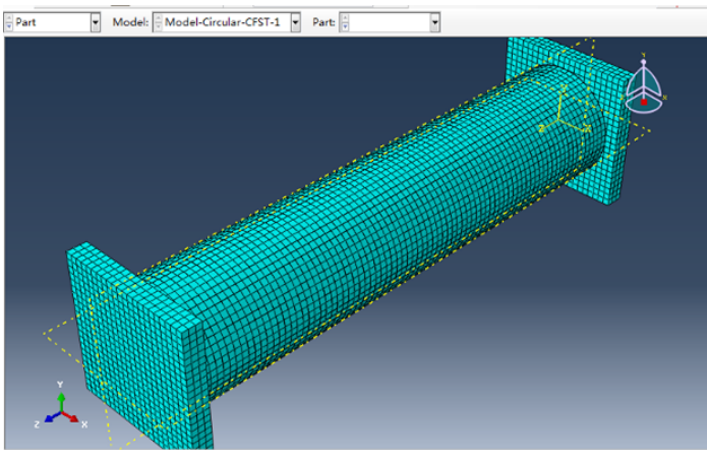

Figure 5 Typical FE model adopted in numerical modeling.

From Figure.2, it can be seen that three loading plates were used at the column ends; therefore, three rigid plates were modeled to simulate these plates, as shown in Figure.5, Figure.6.. Both in the tests and in the FE modeling, the load is applied to the column through the top loading plate. In the test, direct contact existed between the end plates and the end surfaces of the short column; therefore a contact function available in the ABAQUS/Standard solver was used to simulate the interaction between the rigid plate and the column end surface.

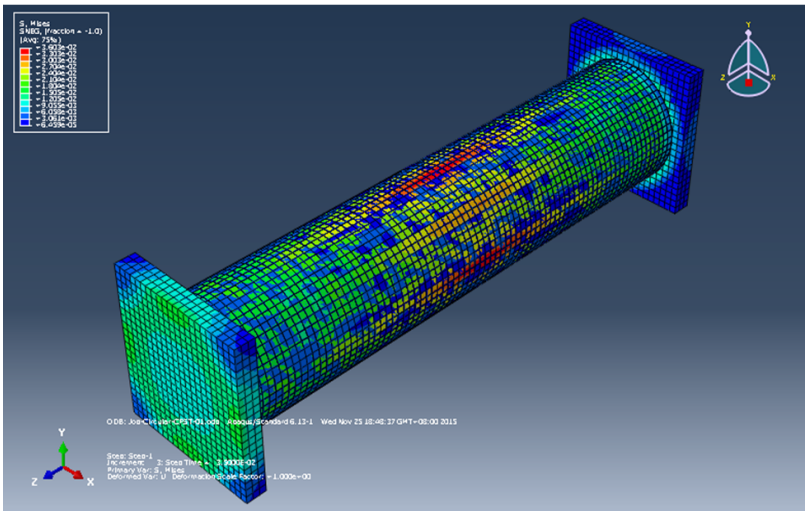

Figure 6. Results of typical FE model

In the FE model, the lower rigid plate contacting the bottom of the column was fixed in all six directions by the reference node, and the upper rigid plate to the top of the column was fixed in five directions and only allowed movement in column axis at the reference node. The column end restraints adopted in the FE model were identical to the testing procedures; no other translations and rotations were observed in tests at both loading plates.

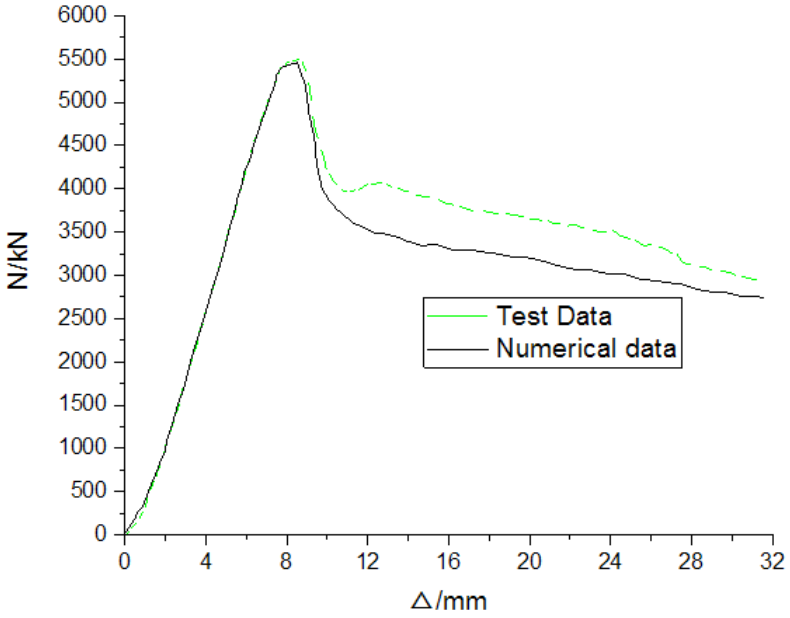

Figure 7. Comparison of maximum loads from experiments and numerical prediction

4.1.Comparison between the numerical and experimental results

The accuracy of the finite element model developed through the ABAQUS/Standard solver combined with the proposed stress–strain model for the confined concrete was verified by comparing the numerical results with the experimental results. The maximum compressive load, load versus column end-

shortening and the column deformed shape were investigated. Figure 5 shows a comparison between the maximum axial compressive loads obtained from the experiments and the maximum axial compressive loads predicted by the finite element models: very good agreements have been obtained. The maximum difference observed between the experimental and numerical results is not exceed 5%.

5. Conclusions

In this paper, three experimental tests on concrete-filled steel tube specimens were conducted under axial load for ultra high strength concrete and basalt fiber reinforced concrete. The objective of the study is to explore the effect of basalt fiber on the axial behavior of steel tube columns filled with high strength concrete. Based on the test results, the following conclusions are reached.

1. Adding steel fibers into concrete core has effect on the failure mode of the CFST columns significantly.

2. The FE numerical method developed via the ABAQUS/ Standard solver could be used to predict the main structural behavior of ultra- strength concrete-filled steel tube columns under axial compressive loads.

Acknowledgements

This work was financially supported by the Natural Science Foundation of Fujian Province, China (Grant No. 2011J01327). This project is supported with the fund from the education fund item of Fujian province(Grant No.JA12292). The authors gratefully acknowledge this support.

References

1. Sakino K, Nakahara H, Morino S, Nishiyama A. (2004) Behavior of centrally loaded concrete-filled steel tube short columns. *Journal of Structural Engineering*, 130(2), p.p.180−188.
2. Shanmugam Ne, Lakshmi B. (2001) State of the art report on steel-concrete composite columns. *J. Constr Steel Res,* 57 (10), p.p.1041–80.
3. H.H. Lee (2007) Shear strength and behavior of steel fiber reinforced concrete columns under seismic loading. *Eng. Struct.,* 29 (7), p.p.1253–1262.
4. T. Fujimoto, A. Mukai, I. Nishiyama (2004) Behavior of eccentrically loaded concrete-filled steel tubular columns, *ASCE J. Struct. Eng.,*130 (2), p.p.203–212.
5. M. Valle, O. Buyukozturk (1993) Behavior of fiber reinforced high-strength concrete under direct shear. *ACI Mater. J.,* 90 (2), p.p.122–133.
6. M. Valle, O. Buyukozturk (1993) Behavior of fiber reinforced high-strength concrete under direct shear. *ACI Mater. J.*, 90 (2) ,p.p.122–133.
7. V.K.R. Kodur (1998) Design equations for evaluating fire resistance of SFRC-Filled HSS columns, *J. Struct. Eng.* ,124 (6), p.p. 671–677.
8. V.K.R. Kodur, T.T. Lie(1996) Fire resistance of circular steel columns filled with steel fiber-reinforced concrete, *J. Struct. Eng.* ,122 (7) ,p.p.776–782.
9. V.K.R. Kodur (1999) Performance-based fire resistance design of concrete-filled steel columns, *J. Constr. Steel Res.,* 51 (1), p.p.21–36.
10. V.K.R. Kodur, T.T. Lie (1995) Fire performance of concrete-filled hollow steel columns, *J. Fire. Prot. Eng.,*7(3), p.p.89–97.
11. T.T. Lie, M. Chabot (1990) A method to predict the fire resistance of circular concrete filled hollow steel columns. *J. Fire. Prot. Eng.* ,2 (4), p.p.111–124.
12. N. Banthia, J.F. Trottier (1995) Test methods for flexural toughness characterization of fiber-reinforced concrete: some concerns and a proposition. *ACI Mater. J.,* 92(2) ,p.p. 48–57.
13. Jean-Francois Trottier (2002) Michael Mahoney, Dean Forgeron, Can synthetic fibers replace welded-wire fabric in slabs-on-grade. *Concr. Int.,* 24 (11) , p.p.59–68.
14. N. Banthia, J.F. Trottier (1995) Test methods for flexural toughness characterization of fiber-reinforced concrete: some concerns and a proposition. *ACI Mater. J.* , p.p.92(2) 48–57
15. Jean-Francois Trottier, Michael Mahoney (2002) Dean Forgeron, Can synthetic fibers replace welded-wire fabric in slabs-on-grade, *Concr. Int.,* 24(11), p.p.59–68.
16. Dylmar Penteadodias, Cleio Thaumatuigo (2005) Fracturetoughness of geopolymeric concretes reinforced with basalt fibers. *Cement and Conerete Composites*, 27, p. p.49-54.
17. Tumadhir Merawi Borhan (2012) Properties of glass concrete reinforced with short basalt fiber. *Materials and Design,* 42, p.p. 265-271